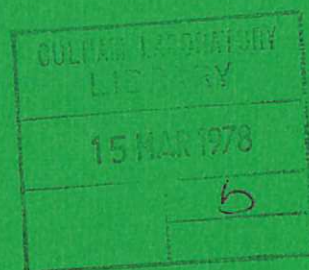




UKAEA

Preprint



STABILITY OF TOKAMAKS

J A WESSON

CULHAM LABORATORY
Abingdon Oxfordshire

1978

This document is intended for publication in a journal or at a conference and is made available on the understanding that extracts or references will not be published prior to publication of the original, without the consent of the authors.

Enquiries about copyright and reproduction should be addressed to the Librarian, UKAEA, Culham Laboratory, Abingdon, Oxfordshire, England

STABILITY OF TOKAMAKS

J.A. Wesson

Culham Laboratory, Abingdon, Oxon., OX14 3DB, UK
(Euratom/UKAEA Fusion Association)

ABSTRACT

A general introduction to the hydromagnetic stability of tokamaks is given and stability theory is related both to experimental results and to reactor requirements.

(Paper presented at the International School of Plasma Physics,
Course on Theory of Magnetically Confined Plasmas, Varenna,
1 - 10 September, 1977.)

January 1978

CONTENTS

I	INTRODUCTION	1
II	IDEAL MODES	5
III	RESISTIVE MODES	7
IV	RELATION OF THEORY AND EXPERIMENT	8
V	HIGH- β EQUILIBRIA	10
VI	THE EFFECT OF PLASMA ELONGATION	11
VII	THE EFFECT OF INCREASED β ON TEARING MODES	12
VIII	STABILITY OF HIGH- β BALLOONING MODES	13
IX	CONCLUSIONS	14

I INTRODUCTION

The aim of these talks is to summarise the overall MHD stability of tokamaks, relating theory to experiment and putting the results into perspective, particularly with regard to reactor requirements.

First then let us recall the objectives, the precise reactor requirements depend upon detailed assumptions but roughly we require

Temperature	$T \approx 10 \text{ keV}$
Particle density	$n \approx 2 \times 10^{14} \text{ cm}^{-3}$
Confinement time	$\tau \approx 1 \text{ sec}$
$\int p d\tau / \int B^2 / 2 d\tau$	$\langle \beta \rangle \approx 10\%$

The β value arises from the values of n and T , together with a technological limitation on the toroidal magnetic field. The present values of τ and β fall short of the required values by a factor of about 20.

Stability requirements impose constraints on the values of β and τ which can be achieved, although the actual limits have not yet been determined. We shall shortly look at the way in which these constraints arise from the different types of instability. Before doing this, however, it will perhaps be worth briefly explaining the nomenclature used to describe the various modes. As might be expected the distinctions are not precise but the following descriptions give the basic ideas.

An initial distinction can be made between ideal and resistive instabilities. Ideal unstable modes are those which would occur if the plasma were infinitely conducting. Resistive modes are those which only occur if the resistivity is finite. Another important concept is that of the resonant surface, that is the surface on which the pitch of the mode matches that of the magnetic field. The position of this surface for a given mode plays a

basic role in determining the nature of the instability. The individual modes will now be described separately.

1. Kink Modes

This term is mainly used for modes which distort the plasma surface. The resonant surface for unstable modes lies outside the plasma. In tokamaks these are potentially the strongest instabilities and are driven by the gradient in the axial current. The term kink mode is also used for the $m = 1$ internal mode because this involves a gross distortion of the plasma inside the $q = 1$ surface.

2. Internal Modes

These are modes which have a resonant surface inside the plasma and the instabilities would occur even if the plasma boundary were not free to move. They are sometimes called interchange modes. The driving force is basically the pressure gradient. For high m -numbers they are localised in radius provided the pressure gradient is not too high. For lower m -numbers these modes are less localised. For sufficiently high β (and therefore high pressure gradients) these modes balloon, that is they are stronger in the region of the cross-section where the magnetic field curvature is worst. As mentioned above the $m = 1$ internal mode is called a kink mode.

3. Axisymmetric Modes

These are modes with no dependence on the toroidal coordinate and are essentially a vertical shift of the whole plasma. They are unstable if the plasma is elongated to too great an extent.

4. Tearing Modes

Are the resistive form of kink modes. Unlike kink modes they have resonant surfaces inside the plasma.

5. Resistive Interchange Modes

These are the resistive form of the ($m > 1$) internal modes.

All these instabilities will be analysed in more detail later, but we now return to the consideration of the constraints they impose.

The constraints on β can be brought out by writing the expression for β in terms of the quantities which determine stability. This may be done as follows:

We use the following expression for average β and β -poloidal

$$\langle \beta \rangle = \frac{\int p \, d\tau}{\int B^2/2 \, d\tau} \quad , \quad \beta_p = \frac{8\pi \int p \, ds}{I^2}$$

where p is the plasma pressure, B is the magnetic field and I is the toroidal current, to obtain

$$\langle \beta \rangle \approx \frac{I^2 \beta_p}{4\pi B_\phi^2 A}$$

where A is the cross-sectional area of the plasma and B_ϕ is a mean value of the toroidal magnetic field.

For most configurations of interest B_ϕ may be expressed by

$$B_\phi \approx \frac{1}{2} q_0 j_{\phi 0} R_0$$

where the subscript zero refers to the magnetic axis, q being the safety factor, j_ϕ the toroidal current density and R_0 the major radius. Using this expression we obtain

$$\langle \beta \rangle = \left(\frac{I}{A j_{\phi 0}} \right)^2 \frac{1}{q_0^2} \frac{A}{\pi R_0^2} \beta_p \quad (1)$$

Each of the factors on the right hand side is constrained by stability considerations. The first factor measures the current carrying capacity of the plasma for a given $j_{\phi 0}$. In order to obtain kink stability it is necessary for j_ϕ to fall off sufficiently rapidly with radius and this then limits the total current and consequently the maximum value of this factor. The second factor, $1/q_0^2$ is limited by internal instabilities. If $q_0 < 1$ then the internal $m = 1$ kink becomes possible and higher m -number internal modes can also limit q_0 . The third factor is increased by having a small aspect ratio and by elongating the plasma to increase the cross-sectional area A . However, this elongation leads to instability of the axisymmetric mode and the greater the elongation the more difficult this is to stabilise. If the plasma is stable to these three categories of mode and the final factor β_p is increased then at some point ballooning of the internal modes will occur and again there is a stability constraint. The factors limiting β may be summarised then as shown below:

$$\langle \beta \rangle = \left(\frac{I}{A_j} \right)^2 \frac{1}{q_0^2} \frac{A}{\pi R_0^2} \beta_P$$

kink
modes
internal
modes
axisymmetric
modes
ballooning
modes

The attribution of the constraint on β_P to ballooning is an oversimplification since there are other factors involved. The introduction of resistivity strengthens the constraints.

The constraints on confinement are less easy to analyse because the processes involved in the transport are not understood. The classical confinement time will scale as I^2 ⁽¹⁾, the current being a measure of the total poloidal flux, which provides the confinement. The non-classical models suggested also give improved confinement with increased current⁽²⁾. Let us ask then what constraints on the total current are imposed by stability requirements. The current may be written in terms of the same factors as equation (1) to give

$$\frac{I}{I_c} = \frac{I}{A_j} \frac{1}{q_0} \frac{A}{\pi R_0^2}$$

where the current I_c , the current in the toroidal magnetic field coil, provides a "cost" normalisation. It is seen that it is again beneficial to have as broad a current profile as is consistent with kink stability, as small a q_0 as is consistent with internal mode stability and as large a plasma area as possible for a given major radius.

Having obtained an overall view of the relation of stability requirements to the reactor objectives we will now look in more detail at the individual modes of instability. It was seen above that an optimized tokamak will be of small aspect-ratio and will probably have a shaped cross-section. However the stability of tokamaks is best understood by first considering the case of circular cross-section and large aspect ratio and proceeding from there to the more difficult problem of optimisation.

The next section will deal with the theory of ideal modes and the following one with resistive modes. Axisymmetric modes will be dealt with in Section VI. A more complete discussion of stability together with the appropriate references may be found in reference (3).

II IDEAL MODES

The potentially most unstable mode is the ideal kink mode. The potential energy of a displacement ξ is given by the low β cylindrical expression

$$\delta W_2 = \frac{\pi^2 B^2}{R_0} \left\{ \int_0^a \left[\left(r \frac{d\xi}{dr} \right)^2 + (m^2 - 1) \xi^2 \right] \left(\frac{n}{m} - \frac{1}{q} \right)^2 r dr \right. \\ \left. + \left[\frac{2}{q_a} \left(\frac{n}{m} - \frac{1}{q_a} \right) + (1 + m\lambda) \left(\frac{n}{m} - \frac{1}{q_a} \right)^2 \right] a^2 \xi_a^2 \right\} \quad (2)$$

where

$$\lambda = \frac{1 + (a/b)^{2m}}{1 - (a/b)^{2m}}$$

a and b are the radii of the plasma and the conducting wall, and perturbations have the form $\exp i(m\theta - n\varphi)$, θ and φ being the poloidal and toroidal angles. The subscript 2 refers to the fact that δW_2 is the second order term in an expansion in (a/R) .

It follows from equation (2) that a necessary requirement for instability is that $q_a < m/n$. Thus, for the usual case with $dj_\varphi/dr < 0$ and $dq/dr > 0$, unstable modes must have a resonant surface in the vacuum region.

An alternative form for δW_2 is

$$\delta W_2 = \pi^2 R_0 \int_0^b \left(B'^2 + B_\theta \left(1 - \frac{nq}{m} \right) \frac{dj_\varphi}{dr} \xi^2 \right) r dr . \quad (3)$$

the integral being taken over the plasma and the vacuum. It is seen that it is the second term which provides the possibility of instability and that the destabilising contribution comes from the current density gradient in the region where $(1 - \frac{nq}{m}) \frac{dj_\varphi}{dr} < 0$. In the usual case dj_φ/dr is negative and the destabilising region lies where $q < \frac{m}{n}$. Thus since for this case dq/dr is positive, unstable region lies inside the resonance surface.

It follows from equation (2) that a necessary requirement for stability is that the current density, $j_{\varphi a}$, at the plasma surface must be zero (or at least not positive) since, for sufficiently large m and n , the resonant surface, r_s , can be chosen arbitrarily close to the plasma surface and the displacement

$$\xi = \frac{m - nq_a}{m - nq} \xi_a$$

gives

$$\delta W_2 = - (2\pi B_{\theta a} \xi_a)^2 \frac{r_s - a}{a} \frac{j_{\varphi a}}{\langle j_{\varphi} \rangle}$$

$\langle j_{\varphi} \rangle$ being the average current density in the plasma.

For lower m , a resonant surface close to the plasma surface leads to more stringent requirements on the smallness of the current gradient in the neighbourhood of the plasma surface. This is illustrated by the results for the two parameter model

$$j_{\varphi} = j_{\varphi 0} \left(1 - \frac{r^2}{a^2} \right)^{\nu}$$

the stability diagram for which is shown in Fig 1. It is seen from this diagram that, provided $q_a > 1$, stability can be obtained for any q_a for a sufficiently peaked current profile.

To complete the description of kink modes it is necessary to add that for the higher m modes stability is easily achieved by removing current from a small region δ inside the plasma surface such that

$$\frac{\delta}{a} \gtrsim \frac{1}{2m}$$

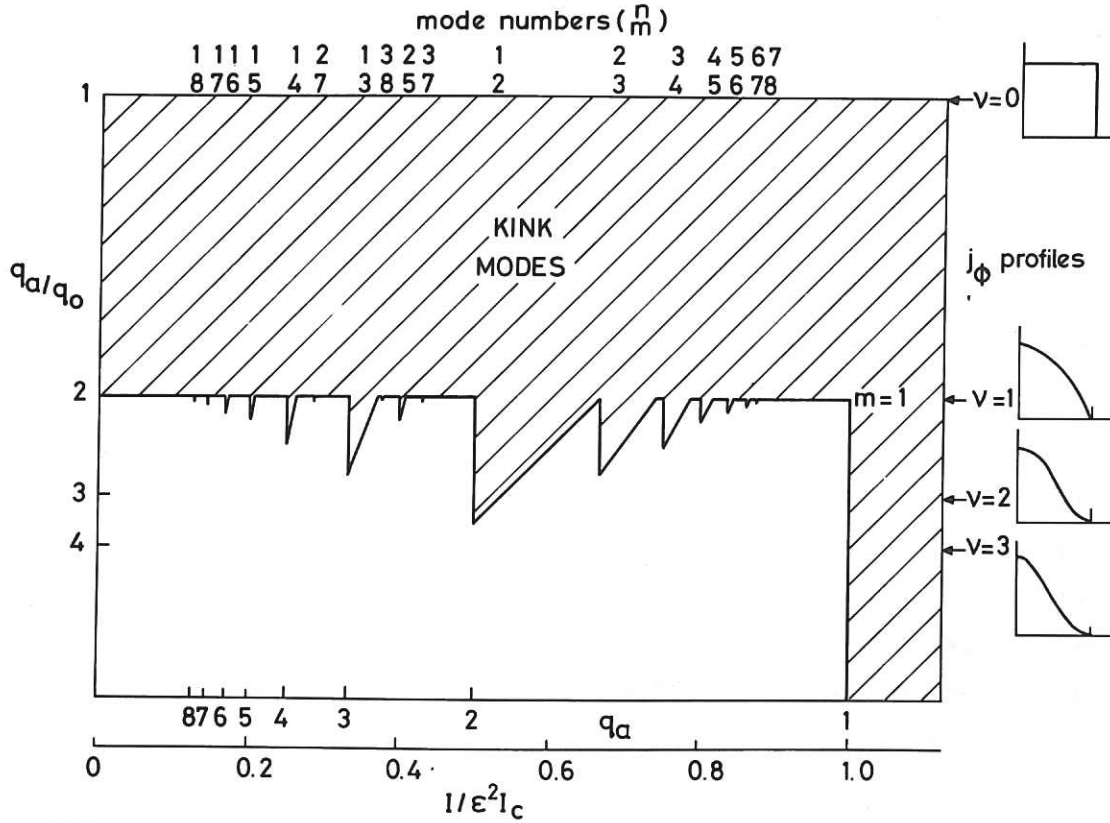


Fig.1 Stability diagram for kink modes for the current distributions $j_\phi = j_{\phi 0} (1 - \frac{r^2}{a^2})^\nu$. The vertical axis measures the peaking of the current as given by q_a/q_0 (which is equal to $\nu + 1$). The horizontal axis measures the total current I expressed as a fraction of $(a/R_0)^2 I_c$ where I_c is the current in the coil producing the toroidal magnetic field. This axis also gives q_a which is inversely proportional to I . The $m = 1$ mode is unstable for $q_a < 1$. The stability region for the other modes is determined principally by the shaping of the current rather than the value of q_a . The differing degrees of current peaking required for each mode is indicated by the sawteeth, the mode numbers (m, n) being given at the top of the figure. For large m the stability requirement is $\nu > 1$.

Turning now to internal modes, for which ξ_a may be put to zero, a necessary condition for the instability of these modes is that the integral in δW_2 must be made sufficiently small that the neglected terms must be retrieved. The stability of internal modes is determined in the order $\delta W_4 \sim \epsilon^4 R_0 \xi^2 B_\phi^2$.

For the $m = 1$ mode, δW_2 can be made to approach zero by a displacement, ξ , approaching $\xi = \text{constant}$ inside the radius at which $q < \frac{1}{n}$ and $\xi = 0$ outside this radius. Modes $m \neq 1$ must be sufficiently localised around the resonant surface for the factor $(\frac{n}{m} - \frac{1}{q})^2$ to make the integral in δW_2 small.

Toroidal calculations for the $m = 1$ mode show a toroidal stabilising effect but it is effective only for rather low values of pressure gradient

inside the surface $q = 1$. Usually therefore stability requires $q_0 > 1$. For high m numbers the appropriate criterion is the Mercier criterion,

$$(-p')(q^2 - 1) + \frac{rB^2}{8} \left(\frac{q'}{q} \right)^2 > 0$$

which gives stability if $q > 1$ everywhere. For a radially decreasing current distribution stability again requires $q_0 > 1$, since the first term dominates at small r .

This stability requirement added to the kink stability diagram gives the diagram of Fig.2. It is important to bear in mind at this point that, even if $q_0 < 1$, the removal of the pressure gradient inside the $q = 1$ surface will restore stability. It might be desirable to accept this small change in order to obtain other advantages. As will be seen later it seems that the plasma configuration adjusts itself to prevent q_0 from going too far below unity.

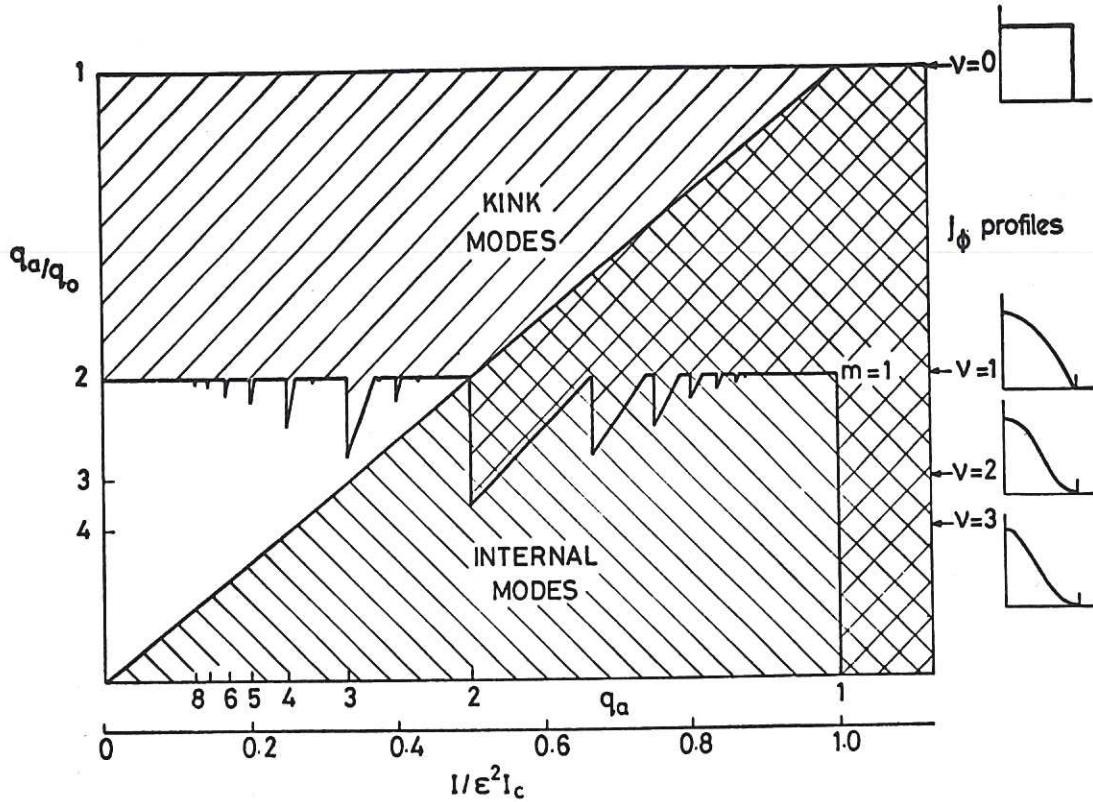


Fig.2 Stability diagram for ideal hydromagnetic modes for the current distribution $j_\phi = j_{\phi 0} (1 - \frac{r^2}{a^2})^\nu$. In this figure the stability requirement, $q_0 > 1$, for the internal modes is added to the kink mode diagram of Fig.1. This criterion covers both the interchange modes and the $m = 1$ internal kink mode. The maximum stable current for this model is obtained with a parabolic current distribution having $q_0 = 1$ and $q_a = 2$.

III RESISTIVE MODES

When resistivity is introduced the internal pressure driven modes are subject to a more stringent requirement. However, if $q > 1$ everywhere, there will be no $q = 1$ surface in the plasma and the $m = 1$ mode will be avoided. Furthermore the modified criterion for localized modes will also be satisfied, that is

$$(-p') \left\{ q^2 - 1 + \frac{q^3 q'}{r^3} \int_0^r \left[\frac{r^3}{q^2} + \frac{2R_0^2 r^2}{B_\phi^2} (-p') \right] dr \right\} > 0$$

The result that kink modes only occur with a resonant surface in the vacuum is also changed by the inclusion of resistivity. Current driven instabilities can now occur with resonant surfaces within the plasma and these modes are called tearing modes. Indeed, in the presence of resistivity the distinction between kink modes and tearing modes is less marked. Both can, in fact, be regarded as resistive modes since for kink modes the resonant surface occurs in vacuum where the resistivity is infinite.

The Euler equation for the δW_2 of equation (2), which covers kink modes, is

$$\frac{d}{dr} \left(\left(\frac{1}{q} - \frac{n}{m} \right)^2 r^3 \frac{d\xi}{dr} \right) - (m^2 - 1) \left(\frac{1}{q} - \frac{n}{m} \right)^2 r \xi = 0$$

This equation may be written in terms of the perturbed radial magnetic field which is given by $\psi = iB_\theta(m - nq)\xi/r$ and it then takes the form

$$\frac{d}{dr} \left[r \frac{d}{dr} (r\psi) \right] - m^2 \psi - \frac{dj_\phi/dr}{(B_\theta/mr^2)(m - nq)} \psi = 0 \quad (4)$$

This is also the equation for neighbouring equilibria:

$$\nabla \times (\underline{j} \times \underline{B})' = 0$$

where the prime indicates to the linearised part and no assumption of perfect conductivity has been made. A mode for which equation (4) is satisfied is marginally stable to tearing modes. In general this equation will not be satisfied and the solution satisfying the regularity condition at $r = 0$ will not allow a continuous matching with the solution satisfying the outer boundary condition. Stability is then determined by the jump in the logarithmic derivative of ψ at the resonant surface,

$$\Delta = \frac{\psi}{r} \frac{d\psi}{dr} \bigg|_{r-\epsilon}^{r+\epsilon},$$

stability being obtained if $\Delta < 0$.

This criterion has been applied to the model of Figs. 1 and 2 and the result is shown in Fig.3. For this model complete stability requires $q_0 > 3$ in order to avoid modes $m = 2$ and 3. The resulting values of β would be 9 times less than that obtained with $q_0 = 1$. However we know that experimental tokamaks do not have to operate with such high q_0 .

Having surveyed the basic stability theory for tokamaks we are now faced with several questions. How does this theory relate to present experiments? How do we investigate higher- β equilibria and what are the problems of achieving higher- β by elongation? How is the large aspect ratio theory of tearing modes modified at smaller aspect-ratio with higher β ? What is the MHD stability limit on the achievable β ? These questions will be considered in turn in the remaining sections.

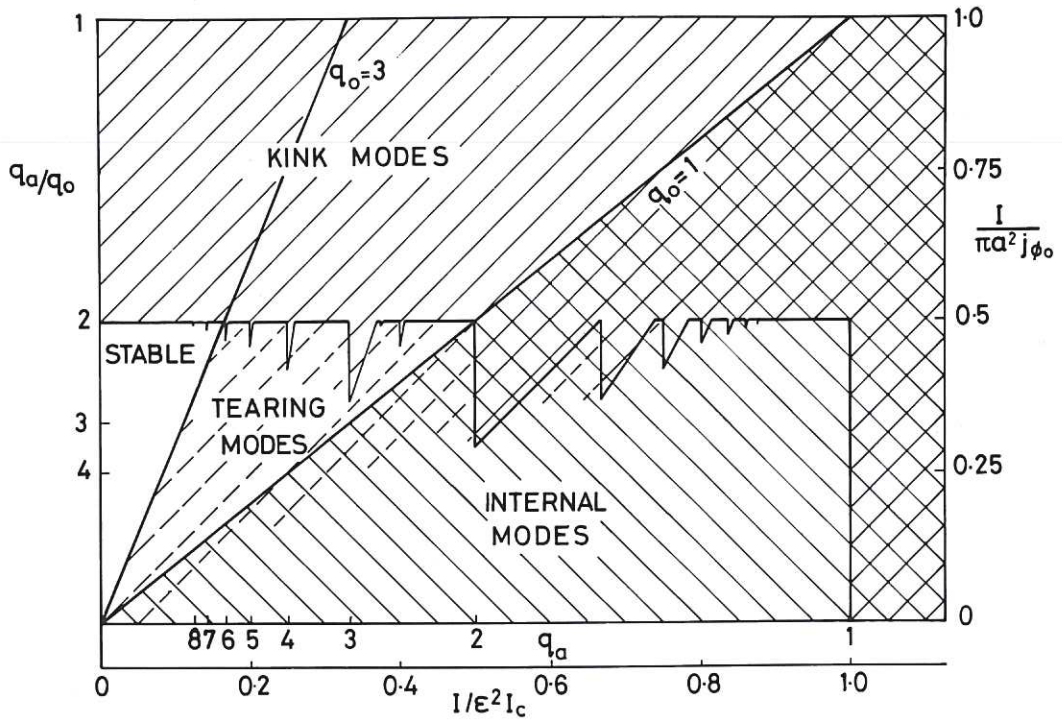


Fig.3 Complete stability diagram for a "standard" tokamak current distribution $j_\phi = j_{\phi 0} (1 - \frac{r^2}{a^2})^\nu$. The diagram gives no indication of the strength of the instabilities but the tearing modes have lower growth rates than the ideal modes and may therefore be more tolerable.

IV RELATION OF THEORY AND EXPERIMENT

First let us look at the variation of energy confinement times as a function of the total current and therefore of q_a . Fig.4 shows some results from T3⁽⁴⁾ from which it is seen that τ_E increases with current up to a certain value and then falls away. The critical value of q_a is between 4 and 5.

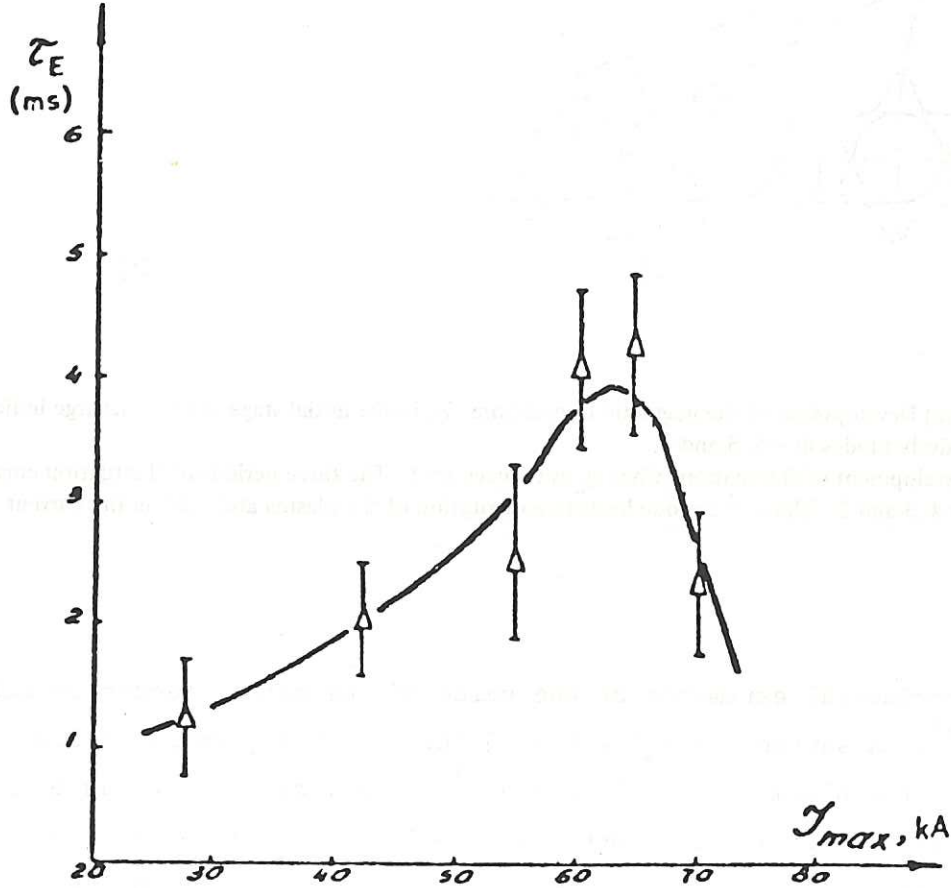


Fig.4 Dependence of τ_E on the value of the discharge current on the T-3 device for $n_e \approx 2 \times 10^{13} \text{ cm}^{-3}$ and $B_\phi = 26 \text{ kG}$.

As the current is increased and q_a falls, magnetic fluctuations occur at the surface and these have been identified by Mirnov and Semenov⁽⁵⁾ as the modes having $m \approx q_a$. A typical result is shown in Fig.5. These modes are identified with the kink or tearing modes which are predicted if sufficient current flows near the edge of the plasma.

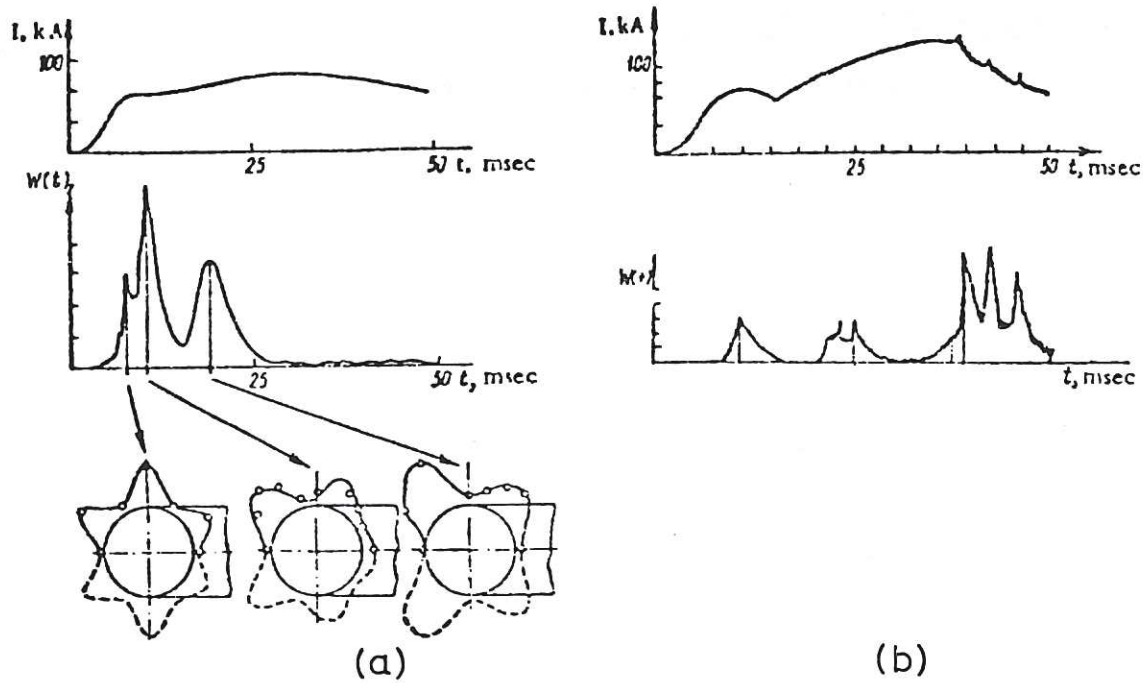


Fig.5 (a) Development of the magnetic fluctuations, W , in the initial stage of the discharge indicating successively modes $m = 6, 5$ and 4 .
 (b) Development of fluctuations when q_a is reduced to 2 . The three periods of fluctuation correspond to $m = 4, 3$ and 2 . The $m = 2$ mode leads to a disruption of the plasma and a fall in the current.

Experimental estimates of the value of the safety factor on axis give $q_0 \approx 1$ ⁽⁶⁾. A sawtooth oscillation of the soft X-ray emission from the central region of the plasma, shown in Fig.6⁽⁷⁾, is believed to be due to a relaxation oscillation. It is thought that ohmic heating leads to a concentration of the current around the magnetic axis making $q_0 < 1$. An instability then occurs which restores $q_0 > 1$. The manner in which this occurs has been investigated by numerical simulation. These calculations reproduce the relaxation oscillations and their physical basis is made clear by the results shown in Fig.7⁽⁸⁾. When q on the magnetic axis falls below unity a magnetic island is formed. The value of q on this island is greater than unity. This island grows, in a manner suggested by Kadomtsev⁽⁹⁾, until it is appropriate to think of the structure as a double helix formed by two magnetic islands. The growing island with $q_0 > 1$ displaces the original "island" with $q_0 < 1$ and this leads to a symmetric configuration with $q_0 > 1$. The whole process then repeats itself.

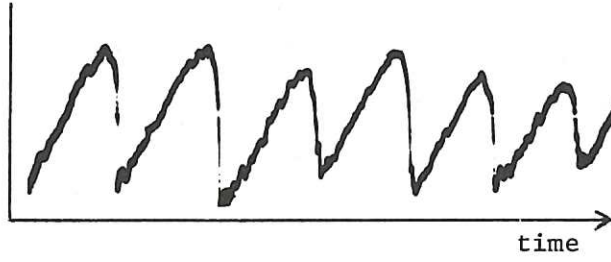


Fig.6 Sawtooth instability. Oscillogram giving the time dependence of the soft X-ray emission for the inner region of the plasma.

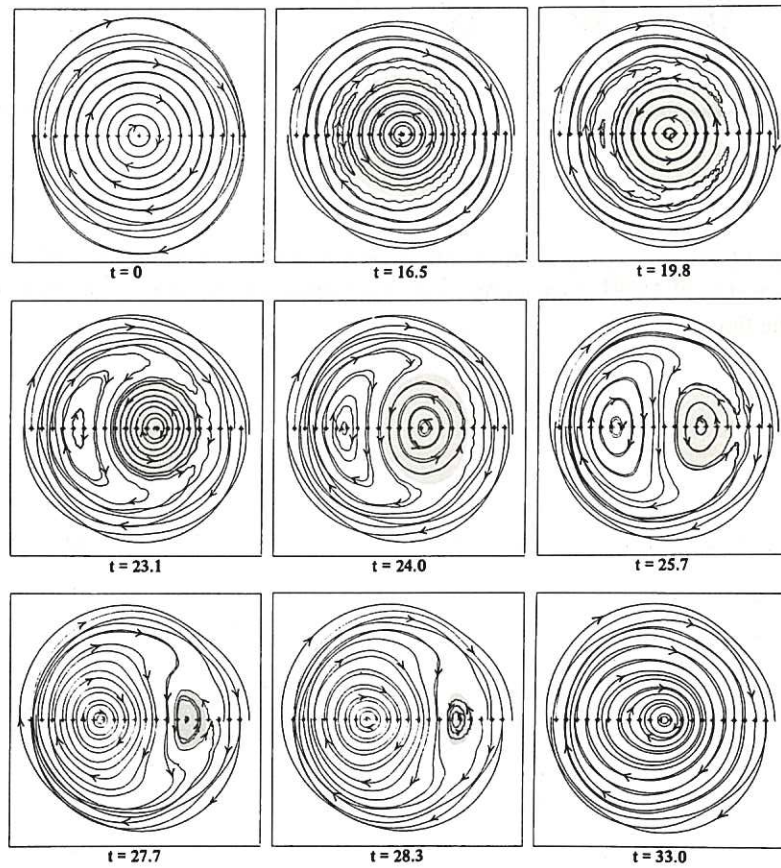


Fig.7 Sawtooth instability. Plots of the transformed magnetic field trajectories. The regions with $q < 1$ are shown shaded. The initially stable configuration becomes unstable as a result of current concentration. An island is formed (having $q > 1$) which grows and displaces the original unstable "island". The island with $q < 1$ decays away. (The small scale variations are not real being due to the computer diagnostic used).

The best confinement is typically obtained with $q_a \sim 4$ and, as we have seen, $q_0 \approx 1$. In the absence of tearing modes, transport would determine the temperature and therefore the current profile. For the types of profile which would then be expected the low m-number tearing modes would be unstable. Evidence for such low m-number modes has in fact been observed and an example is shown in Fig.8⁽¹⁰⁾.

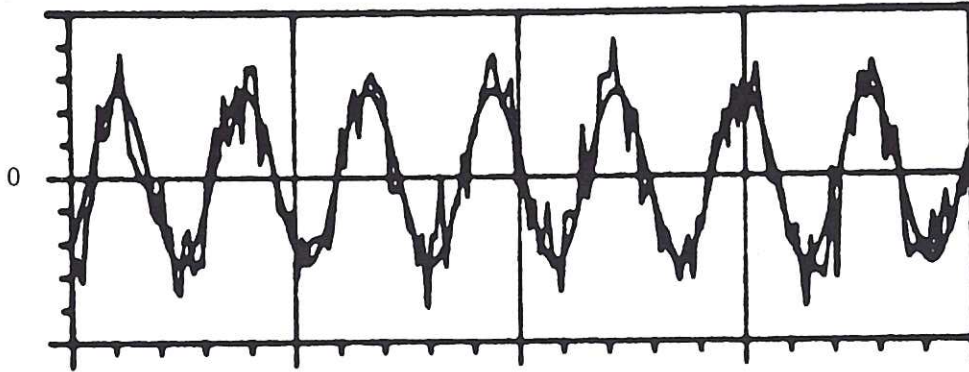


Fig.8 Fluctuating component of soft X-ray signal showing an $m = 2$ oscillation, observed in PLT⁽¹⁰⁾. Signal represents line integrated emission. The total time in the figure is 2 ms.

It appears then that the effect of tearing modes is such that it is preferable for confinement to accept their non-linear consequences in order to obtain a higher current. This would correspond, in Fig.3, to working around the $q_0 = 1$ line with $q_a \sim 4$ where the $m = 1$ internal kink and $m = 2$ and $m = 3$ tearing modes are predicted.

The growth of tearing modes will lead to island formation as illustrated in Fig.9. This results in a reduction over this region of the destabilising current gradient. It has been shown⁽¹¹⁾ that, if the current profile is adjusted, stable configurations with $q_0 \approx 1$ and q_a as low as 2.6 are possible. The resulting current profile is shown in Fig.10. If, however, such profiles are obtained as a result of the non-linear effects of instabilities, the resulting additional transport would have to be tolerated.

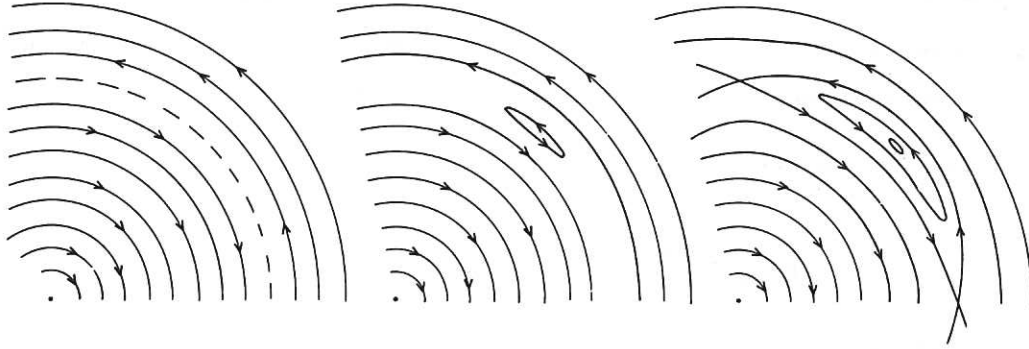


Fig.9 Illustrating the way in which magnetic islands are formed at a rational surface. The field lines plotted are those of $B^* = B_r \hat{r} + (B_\theta - \frac{2\pi r}{L} B_z) \hat{\theta}$ where L is the periodicity length in z .

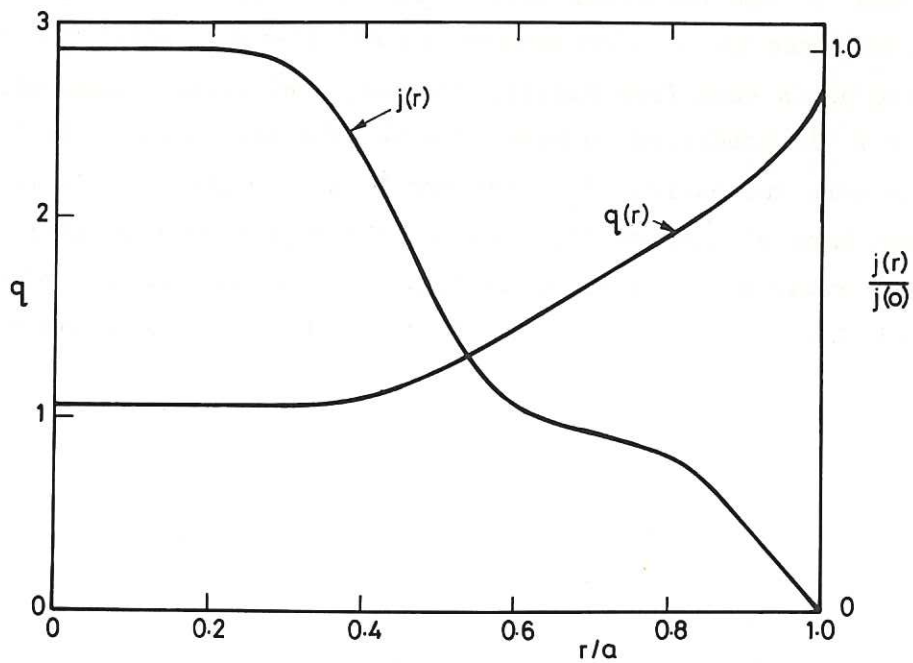


Fig.10 Showing the current and q profiles for a configuration (with no conducting shell) which has been designed to give stability for all low m -number tearing and kink modes.

V HIGH- β EQUILIBRIA

It was pointed out by Mukhovatov and Shafranov in 1971⁽¹²⁾ that there is no theoretical limit to the equilibrium β that can be obtained in a tokamak. However some care is needed to obtain an equilibrium model which allows the control necessary for the optimisation of β .

The equilibrium equation for the poloidal flux ψ is

$$R \frac{\partial}{\partial R} \frac{1}{R} \frac{\partial \psi}{\partial R} + \frac{\partial^2 \psi}{\partial z^2} = - R^2 p' - f f' (= - R j_\varphi)$$

with $p = p(\psi)$ and $f = f(\psi)$. A simple choice which gives a roughly parabolic current distribution at large aspect ratio is $p' \propto \psi$ and $f f' \propto \psi$. For an elliptical plasma with $q_0 = 1$ this gives, at large aspect ratio,

$$\% \beta \approx 20 \beta_p (a/R_0)^2 (b/a) \quad (5)$$

where b and a are the minor axis of the ellipse. However for this model the actual increase in β with decreasing aspect-ratio falls off at small aspect ratio as is seen from Fig.11. Whereas a circular plasma with $\beta_p = 1$ and $R_0/a = 2$ is predicted to have $\beta = 5\%$ the actual value is less than 2%. Furthermore increasing β_p does not lead to higher β in this model⁽¹³⁾. On the other hand elongation does lead to the improvement predicted by the large aspect ratio model as shown in Fig.12. However the β value for $\beta_p = 1$ and $R/a = b/a = 2$ is only 3% compared to the 10% predicted by equation (5).

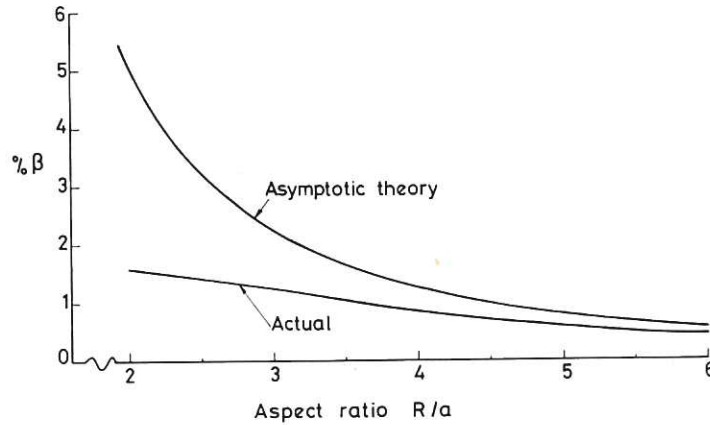


Fig.11 β , expressed as a percentage, as a function of aspect ratio for a circular plasma with $p' \propto \psi$, $f' = 0$ and $q_0 = 1$.

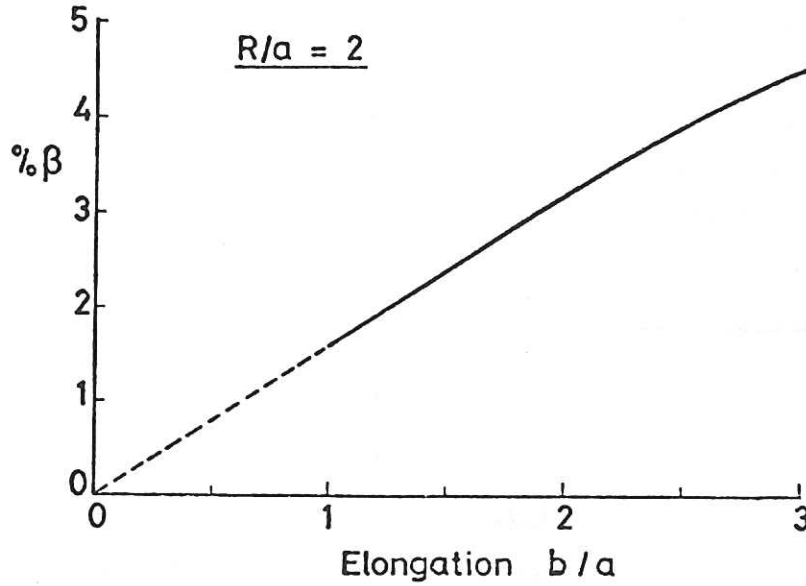


Fig.12 β , expressed as a percentage, for an elliptical plasma as a function of the ratio of the major and minor axis. The aspect ratio $R/a = 2$ with $p' \propto \psi$, $f' = 0$ and $q_0 = 1$.

A set of equilibria which allows the independent variation of β, β_p and q_0 may be obtained from the following model⁽¹⁴⁾

$$R^2 p' = \alpha_1 R^2 \psi + \alpha_2 R^2 \psi^2$$

$$ff' = -\alpha_2 R_0^2 \psi^2 - \alpha^3 \psi^3$$

so that

$$Rj_\varphi = \alpha_1 R^2 \psi + \alpha_2 (R^2 - R_0^2) \psi^2 - \alpha^3 \psi^3$$

The quadratic term allows substitution of kinetic pressure for toroidal magnetic field. The last term enables toroidal current to be removed from the region around the magnetic axis (maximum ψ), and therefore q_0 to be increased, in a similar way to that which occurs experimentally as described in Section IV.

A general view of the equilibria allowed by this model is given by the (β, β_p) plot of Fig.13, which gives some results for the proposed JET configuration⁽¹⁴⁾. At any point in the (β, β_p) plane the value of q_0 can be varied. The current I_1 corresponds to $1.43 \times B_\varphi$ Mamps in JET, where B_φ is in teslas. If β is increased by increasing the total current at a given β_p then $\beta \propto I^2$. The resulting increased current gradients are accompanied by lower values of q_a and it would be expected that this will lead to kink instability. If, on the otherhand, β is increased at a

given current by increasing β_p , the improvement in β is only linear but the value of q_a is increased and this might lead to some improvement in kink stability. Before moving to a discussion of the dependence of stability on β for a given plasma shape we shall first consider a destabilising effect which arises if higher β is obtained by elongation of the plasmas.

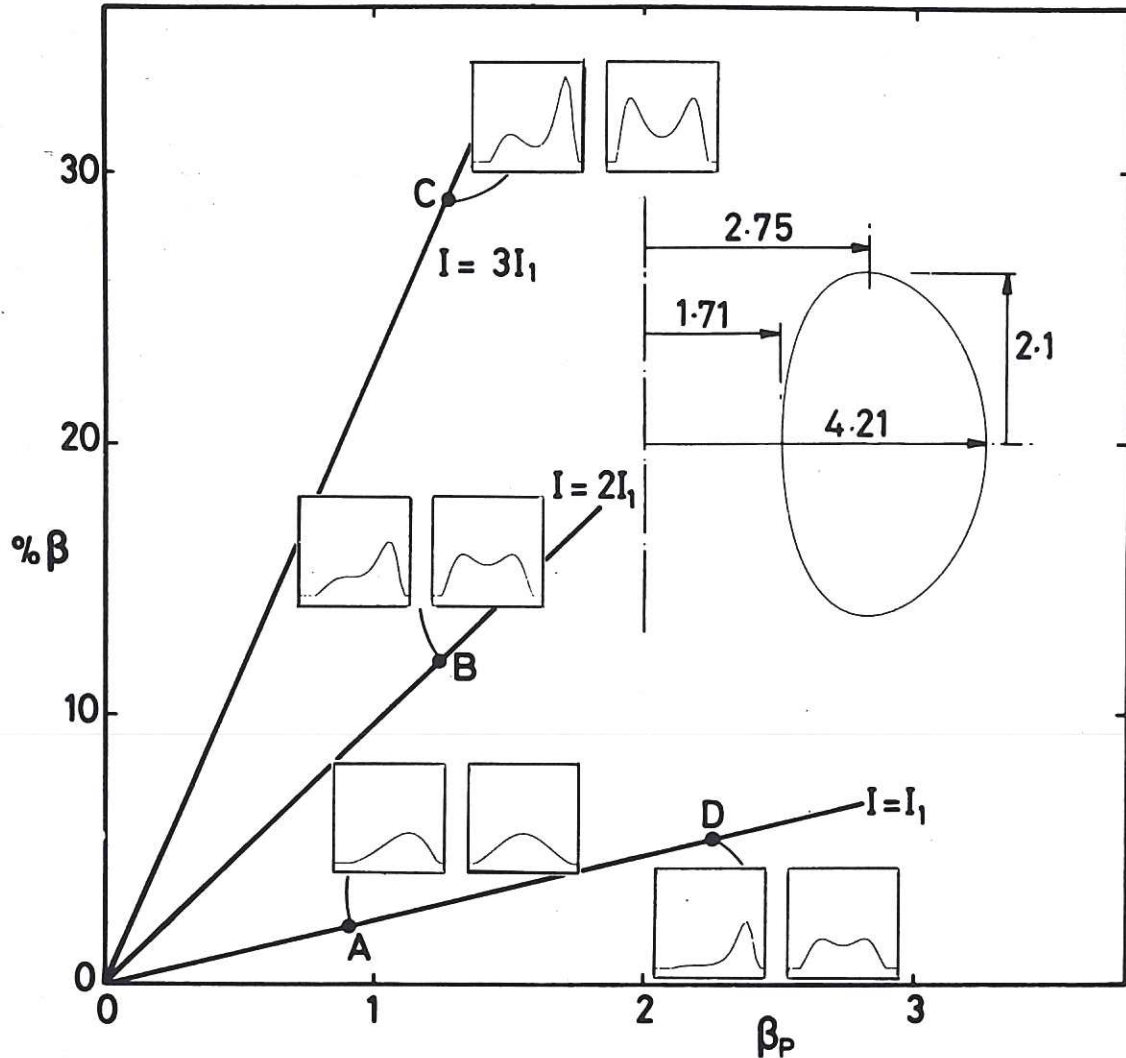


Fig.13 Equilibrium diagram. Each point in the (β, β_p) plane corresponds to a given current, and lines corresponding to three currents I_1 , $2I_1$ and $3I_1$ are shown. ($I_1 = 1.43 B_{\phi 1}$ M amps if $B_{\phi 1}$, the toroidal magnetic field at $R = 3$, is in teslas and the dimensions shown are in metres). Current distributions are shown for four chosen equilibria. In each case the left-hand figures show the current distribution in the horizontal midplane and the right-hand figures show it along a vertical line through the magnetic axis. The current distributions shown are four equilibria with $q_0 = 1$ but it is possible to vary q_0 while remaining at a fixed point in the diagram by redistributing the current. The current profiles all have the same scale.

VI THE EFFECT OF PLASMA ELONGATION

A variety of arguments has been made concerning the merits of shaped plasmas but the most important case for elongation appears to be that, as seen from equation (1), it allows a higher equilibrium β for a given current profile and a given value of q on the magnetic axis.

However elongation of the plasma leads to the introduction of another possible type of instability, the axisymmetric, or $n = 0$, mode. This mode is basically a vertical shift of the plasma.

For an elliptical plasma with a constant current density surrounded by a perfectly conducting shell the stability criterion is⁽¹⁴⁾

$$\frac{b - a}{b + a} < \left(\frac{b + a}{b' + a'} \right)^2 \quad (6)$$

where b' and a' are the semi-axes of the shell. For $b/a = 2$ the shell position required for stability is $(b + a)/(b' + a') > 0.58$. In practice the conductors used for stabilisation are likely to have a finite conductivity. To estimate the effect of this, the shell in the example given above can be made finitely conducting. The $n = 0$ mode is then always unstable. Provided criterion (6) is well satisfied the growth rate is given by⁽³⁾

$$\gamma = 1/D\tau_R$$

where

$$D = \frac{b + a}{b - a} \left(\frac{b + a}{b' + a'} \right)^2 - 1 ,$$

$D > 0$ being the criterion (6), and τ_R is the resistive time of the conducting shell. This remaining instability would require feedback stabilisation.

VII THE EFFECT OF INCREASED β ON TEARING MODES

The full treatment of tearing modes requires first of all a calculation of the jump Δ as described in section III and secondly the matching of this jump to the solutions obtained in a resistive layer around the resonant surface. When compressibility is taken into account the solution in the resistive layer is altered and the resulting stability criterion is changed from $\Delta > 0$ to $\Delta > \Delta_c$ where Δ_c increases with β . The value of Δ_c , derived by Glasser, Greene and Johnson, is⁽¹⁵⁾

$$\Delta_c = 1.54 \frac{r}{a} \left[\epsilon S \frac{m a \frac{dq}{dr}}{q^2} / (1 + 2q^2)^{\frac{1}{2}} \right]^{\frac{1}{3}} \times$$

$$\left(\left[\frac{2}{B_\phi^2} \frac{q^2 (-dp/dr)}{r (dq/dr)^2} \left\{ q^2 - 1 + \frac{q^3}{r^3} \frac{dq}{dr} \int_0^r \left[\frac{r^3}{q^2} + \frac{2R_o^2 r^2}{B_\phi^2} \left(-\frac{dp}{dr} \right) dr \right] \right\} \right]^{\frac{5}{6}} \right)$$

This criterion can be applied to the model of Fig.3 to find the effect on the stability diagram⁽¹⁶⁾. The pressure is taken to be given by

$$\frac{dp}{dr} = -\beta_p j_\phi B_\theta$$

and the parameter determining stability turns out to be

$$\Lambda = \beta_p^{\frac{5}{6}} \epsilon^{\frac{1}{3}} S^{\frac{1}{3}}.$$

For present experiments Λ is of the order 3-10 and a tokamak with an aspect ratio of 2.5 and $T_e \sim 4$ keV would have a Λ of about 30.

It is found that for $\Lambda \gtrsim 3$ the $m = 3$ mode is predicted to be stabilised over most of the previously unstable region in the stability diagram. This leaves the $m = 2$ mode and the results for this mode are shown in Fig.14. It is seen that a considerable improvement is predicted as Λ is increased and that stable operation of $q_0 \approx 1$ is possible for $\Lambda \gtrsim 30$.

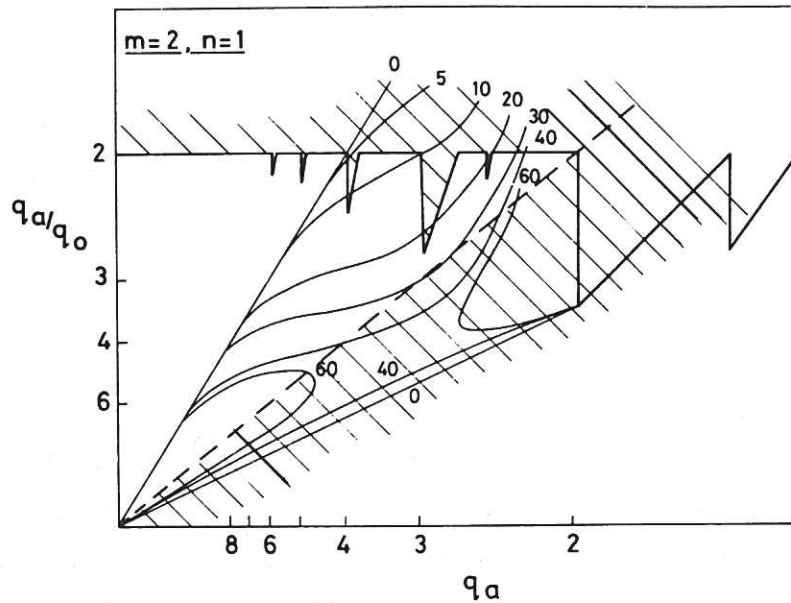


Fig.14 Stability diagram for $m = 2, n = 1$ mode for various values of Λ . This is the dominant tearing mode and the diagram shows the improved overall stability, over that of Fig.3, as Λ is increased.

Further analysis of these modes is necessary both to include the effects of finite Larmor radius and to extend the theory to the collisionless regime.

VIII STABILITY OF HIGH- β BALLOONING MODES

The theory of stability outlined in sections II and III loses its validity as β is increased. The principal reason is that the increased energy available to drive instability is sufficient to produce significant bending of the magnetic field lines. This means that perturbations can vary strongly along the magnetic field and can be large on the side of the plasma furthest from the major axis, where the magnetic field curvature is worst, and small on the side close to the major axis, where the curvature is favourable. This phenomenon is called ballooning.

We shall look shortly at some numerical calculations carried out to study this effect but it will be instructive first to look at a simple model of the physics of ballooning.

If we take the ballooning to be strong so that the displacement is large in the region of bad curvature then the potential energy available to drive the instability is proportional to

$$\frac{1}{R} \frac{dp}{dr} \xi^2$$

where ξ is the displacement and R the radius of curvature of the magnetic field line which for the present purpose is adequately measured by the major radius of the torus. The energy increase resulting from the line bending is roughly proportional to $k_{\parallel}^2 B_{\phi}^2 \xi^2$ or

$$\left(\frac{2\pi}{l}\right)^2 B_{\phi}^2 \xi^2$$

where l is the length of the field line over which the bending occurs. An approximate stability condition will therefore take the form

$$\frac{dp}{dr} < c \left(\frac{2\pi}{l}\right)^2 R \frac{B_{\phi}^2}{2}$$

or

$$r \frac{d\beta}{dr} < c \frac{r}{R} \left(\frac{2\pi R}{l}\right)^2$$

where c is a constant of order unity. It is tempting to make the further step of putting $l \approx 2\pi Rq$ and obtain for the critical β the ordering

$$\beta \sim \epsilon/q^2 .$$

However this would be misleading since the effective value of ℓ can be much shorter than this, and in any case a precise numerical calculation of stability is required.

Two dimensional numerical calculations have been carried out for some of the equilibria described in Section V and illustrated in Fig.13⁽¹⁴⁾. The growth rates of the first three toroidal modes, that is $n = 1, 2$ and 3 , have been calculated for the configuration D, which has $\beta = 5.4\%$ and B, which has $\beta = 12\%$. The plasma was taken to have a conducting wall on its surface and consequently only the internal modes are allowed. The results are shown in Fig.15. It is seen that in both these cases the modes are found to be stable for sufficiently high q_0 . An eigenfunction for the $n = 3$ mode is shown in Fig.16 to illustrate the effect of ballooning. The vectors show the local poloidal displacement of the plasma. High m-modes cannot be treated by this type of calculation and a method of treating these separately has been devised^{(17),(18)}.

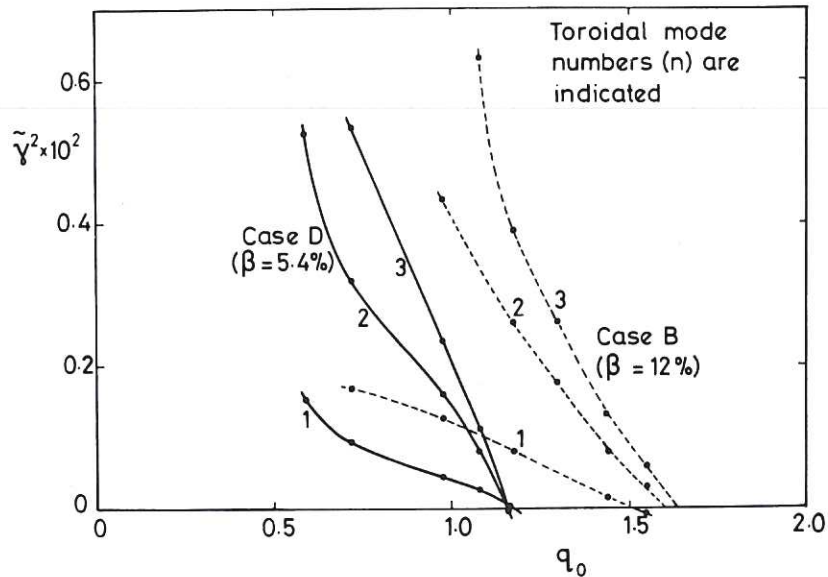


Fig.15 Stability diagram for internal modes giving the square of the dimensionless growth rate $\tilde{\gamma} (= \frac{1}{2} \gamma R_1 / (B_{\phi_1} / \sqrt{\rho}))$ where R_1 is the radius of the point $R = 3$ in the mid-plane of Fig.13 and B_{ϕ_1} is the toroidal magnetic field at that point) against q_0 , the value of q on the magnetic axis. The full lines give the growth rates of the modes with toroidal mode numbers $n = 1, 2$ and 3 for equilibrium D of Fig.13 and the broken lines give the corresponding growth rates for equilibrium B.

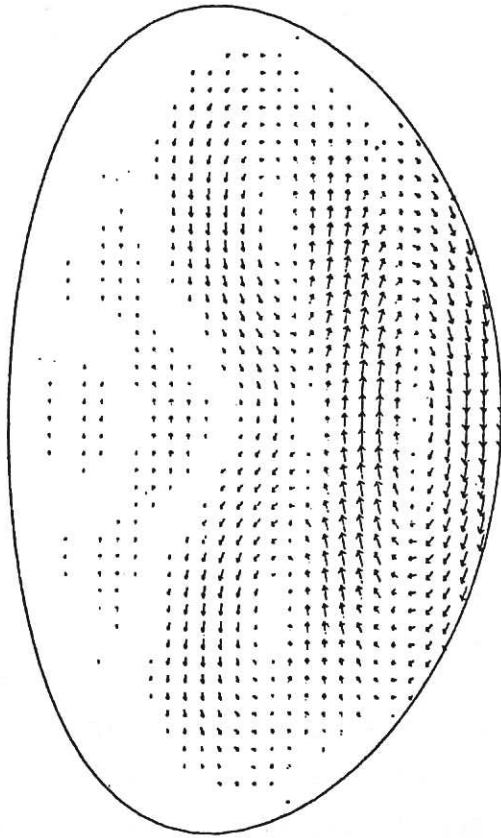


Fig.16 Eigenfunction for $n = 3$ mode illustrating the effect of ballooning. The vectors give the local poloidal displacement.

IX CONCLUSIONS

The stability properties of tokamaks at large aspect ratio and low- β are fairly well understood and there is a reasonable connection between theory and experiment. At higher β the theory is less advanced and there is no experimental evidence. Initial ideal mhd calculations for configurations with $\beta \sim 10\%$ look promising but it is necessary to determine the stability of modes with high mode numbers, the stability against resistive modes and the non-linear consequences of any modes which may be unstable.

ACKNOWLEDGEMENT

The author would like to thank Alan Sykes for providing the computation results for Figs.11 and 12 and Bruno Coppi for helpful discussions on ballooning modes.

REFERENCES

- (1) FURTH, H.P. Nuc. Fus. 15 (1975), 487
- (2) Status and Objectives of Tokamak Systems for Fusion Research, U.S. Atomic Energy Commission, WASH-1295 (1974)
- (3) WESSON, J.A., Hydromagnetic Stability of Tokamaks. Nuc. Fus. 28 (1978), 87.
- (4) MIRNOV, S.V. Nuc. Fus. 9 (1969), 57.
- (5) MIRNOV, S.V. and SEMENOV, I.B. Soviet Atomic Energy 30 (1971) 22-29 (From Atomnaya Energiya 30 (1971) 20).
- (6) KAKISHIMA, K., TOMINAYA, T., TOHYAMA, H. and YOSHIKAWA, S., Phys. Rev. Letts. 36, (1976), 142.
- (7) T.F.R. Group, Proc. 7th European Conf. on Controlled Fusion and Plasma Physics (1975), Vol.II, p.1.
- (8) SYKES, A., and WESSON, J.A., Phys. Rev. Letts 37 (1976), 140.
- (9) KADOMTSEV, B.B., Fiz. Plasmy 1 (1975), 710.
- (10) GROVE et al. Proc. 6th International Conf. on Plasma Physics and Contr. Nuc. Fus. Res. Berchtesgaden (1976), Vol.I, p.21.
- (11) GLASSER, A.H., FURTH, M.P. and RUTHERFORD, P.M. Phys. Rev. Letts. 38, (1977) 234
- (12) MIKHOVATOV, V.S. and SHAFRANOV, V.D. Nuc. Fus. 11, (1971), 605.
- (13) GIBSON, A. and GREEN, B.J. Nuc. Fus. 16 (1976), 521.
- (14) SYKES, A., WESSON, J.A. and COX, J.P. Phys. Rev. Letts. 39 (1977), 757.
- (15) GLASSER, A.H., GREFNE, J.H. and JOHNSON, J.L. Phys. Fluids 19 (1976), 567.
- (16) HASTIE, R.J., SYKES, A., TURNER, M. and WESSON, J.A., Nuc. Fus. 17 (1977) 515.
- (17) COPPI, B. Phys. Rev. Letts 39 (1977), 939.
- (18) DOBROTT, D., NELSON, D.B., GREFNE, J.M., GLASSER, A.H., CHANCE, M.S., and FRIEMAN, E.A. Phys. Rev. Letts 39 (1977), 943.

© 2006 The Authors
Journal compilation © 2006 Blackwell Publishing Ltd